Int. J. Electrochem. Sci., 11 **(2016)** 1327 - 1336

International Journal of
ELECTROCHEMICAL
SCIENCE
www.electrochemsci.org

Voltammetric Determination of Butyl Hydroxy Anisd Based on the Enhanced Effect of Gold Nanorods Assembled on a Poly-L-cysteine Film Electrode

Yinghua Deng[1], *Kaiping Luo*[2], *Guishen Liu*[3], *Xiaodong Hou*[3], *Yina Huang*[3], *Chunya Li*[2,*]

[1] Hubei key laboratory of purification and application of plant anti-cancer active ingredients, Hubei University of Education, Wuhan 430205, China
[2] Key Laboratory of Analytical Chemistry of the State Ethnic Affairs Commission, College of Chemistry and Materials Science, South-Central University for Nationalities, Wuhan 430074, China
[3] Chaozhou Quality and Measurement Supervision and Inspection Institute, Chaozhou 521011, China
[*]E-mail: lichychem@163.com

Received: 11 October 2015 / *Accepted:* 12 December 2015 / *Published:* 1 January 2016

Polymerization of L-cysteine was performed on a glassy carbon electrode surface using cyclic voltammetric scanning from -0.2 V to 2.0 V. After being immersed in a gold nanorods solution over one night, a gold nanorod modified poly-L-cysteine film electrode (GNRs/poly-L-cysteine/GCE) was successfully fabricated. The assembling of gold nanorods onto the poly-L-cysteine film electrode was confirmed with scanning electron microscope and electrochemical impedance spectroscopy, respectively. Voltammetric behaviors of butyl hydroxy anisd (BHA) at the GNRs/poly-L-cysteine/GCE were investigated. Compared to the bare GCE, the GNRs/poly-L-cysteine/GCE exhibited significantly enhanced effects on the oxidation peak current of BHA. Square wave voltammetric responses were used for the BHA determination. Under optimized conditions, it was found that the oxidation peak current is linearly related to the BHA concentration in the range of $5.0 \times 10^{-8} \sim 7.0 \times 10^{-6}$ mol L^{-1}. The detection limit was calculated to be 8.5×10^{-9} mol L^{-1} (S/N=3). The practical application of the GNRs/poly-L-cysteine/GCE was demonstrated by determining BHA in oil samples.

Keywords: Butyl hydroxy anisd; gold nanorod; poly-L-cysteine; voltammetry.

1. INTRODUCTION

Antioxidants are a typical type of compounds that can be used to retard oxidative degradation processes in food and pharmaceutical industry [1]. As the oxidative free radicals can be removed, antioxidants are also demonstrated an effective component in anti-aging for humans [2]. Although some natural antioxidants such as vitamin A, vitamin E and polyphenol possess superior properties,

unfortunately, the instability and high cost often restrict their applications. As a result, many synthetic phenolic antioxidants, commonly butyl hydroxy anisd, butylated hydroxytoluene and butylated hydroquinone have been provided as a substitute [3, 4]. Nevertheless, an excessive using of these antioxidants will be harmful to human health due that they have been verified to possess adverse effect on the activity of liver microsomal fraction [5, 6]. Therefore, their safe usage levels are strictly restricted. For instance, the permitted levels of phenolic antioxidants are less than 200 mg kg^{-1} according to the Food and Drug Administration and the European Union [7]. To develop a practical method for these phenolic antioxidants determination is critically important to monitor the adequate using of them. Various analytical approaches including spectrophotometry [8], high-performance liquid chromatography [9, 10], chromatography coupled with mass spectrometry [11] and electrochemical sensors [12 - 15] have been developed for the determination of phenolic antioxidants. Among those means, electrochemical sensors that possess some superior properties including high sensitivity and selectivity, facilely fabricated, simply miniaturized and low cost, have been demonstrated to be valuable tools for the practical detection of phenolic antioxidants. Thus, to fabricate an electrochemical sensor for butyl hydroxy anisd determination is also apparently desired for human beings to keep them out from the damage of phenolic oxidants.

Up to date, there have been many attempts to synthesize nanomaterials based on gold nanorods, and to develop their utilizations in the fields of electrochemical sensing, biosensing, energy, and drug delivery [16 - 18]. Gold nanorods have also been proved to be an enhanced element for amplifying the electrochemical sensing signals. Based on well-dispersed graphene/gold nanorod composites, an electrochemical sensor for the sensitive determination of ractopamine was fabricated [19]. By introducing a host-guest binding reaction into the assembly process of a gold nanorod superstructure, the signal for the electrochemical immunosensing was significantly amplified [20]. Multifunctional "nano-pearl-necklaces" based on gold nanorod/Fe_3O_4 nanoparticle were used as an MRI and fluorescence imaging agent to target cancer cells, and also demonstrated to be effective in photothermal therapy [21]. Herein, gold nanorods were assembled onto a poly-L-cysteine film electrode surface to fabricate a novel electrochemical sensor for butyl hydroxy anisd. The morphology of the poly-L-cysteine film electrode decorating gold nanorods was characterized with scanning electron microscope. The interfacial properties of the obtained GNRs/poly-L-cysteine/GCE was explored by electrochemical impedance spectroscopy. Electrochemical behaviors of butyl hydroxy anisd at the GNRs/poly-L-cysteine/GCE were investigated by using voltammetry. The results indicated that GNRs/poly-L-cysteine composite film can significantly enhanced the voltammetric response of butyl hydroxy anisd, and thus employed for its determination. The practical application of the GNRs/poly-L-cysteine/GCE was successfully demonstrated by determining butyl hydroxy anisd in oil samples.

2. EXPERIMENTALS

2.1 Apparatus and Reagents

All electrochemical experiments were performed on CHI660D Electrochemical Workstation (Chenhua, Shanghai, China). A commonly used three-electrode system including a glassy carbon

working electrode (Gaossunion, Wuhan, China), a platinum wire auxiliary electrode, and a saturated calomel reference electrode (SCE) was employed for electrochemical measuring. Scanning electron microscopic (SEM) images were carried on a Sirion 200 microscope (FEI). Transmission electron microscopic (TEM) image was obtained on an FEI Tecnai G220S-TWIN instrument (FEI Company, Netherlands) operating at an acceleration voltage of 200 kV.

Aurichlorohydric acid, silver nitrate, cetyl trimethyl ammonium bromide, and sodium borohydride were purchased from Sinopharm Chemical Reagent Co., Ltd. (Shanghai, China). Butyl hydroxy anisd was brought from Aladdin (Shanghai, China). Phosphate buffer (0.1 mol L^{-1}) was prepared by mixing the standard solution of KH_2PO_4 and Na_2HPO_4. 0.1 mol L^{-1} NaOH and H_3PO_4 were used to adjust pH values. Electrochemical impedance spectroscopy was measured in 0.1 mol L^{-1} KCl containing 5.0 mmol L^{-1} $K_3Fe(CN)_6/K_4Fe(CN)_6$ (1:1). The frequency is ranged from 1×10^5 to 1×10^{-1} Hz with the perturbation amplitude of 5 mV. Other reagents were of analytical grade, and were used without further purification.

2.2 Preparation of gold nanorods

According to previous report [16], a typical procedure for gold nanorods preparation was presented as following:

Firstly, $HAuCl_4$ (1 mL, 0.5 mmol L^{-1}) was thoroughly mixed with cetyl trimethylammonium bromide (CTAB, 1 mL, 0.2 mol L^{-1}). Then, freshly prepared $NaBH_4$ (0.12 mL, 0.01 mol L^{-1}) solution was injected into the system to reduce $HAuCl_4$ to produce gold seeds. Subsequently, gold seeds (40 μL) were homogeneously mixed with $HAuCl_4$ (6 mL, 5 mmol L^{-1}), CTAB (30 mL, 0.2 5 mol L^{-1}), $AgNO_3$ (75 uL, 0.1 mol L^{-1}), HCl (67 μL, 1.2 mol L^{-1}). After that, 3.5 mL ascorbic acid (0.01 mol L^{-1}) was spiked into the above system. Stirring for 10 min, the reaction was maintained at room temperature for 24 h. Gold nanorods were simply collected by centrifugation, and washed with ultrapure water.

2.3 Fabrication of the GNRs/poly-L-cysteine/GCE

A glassy carbon electrode was polished with alumina slurries and thoroughly rinsed with ultrapure water. Then, it was successively ultrasonicated in nitric acid, ethanol, and water, and allowed to dry at room temperature. Cyclic voltammetric scanning in a L-cysteine solution (6 mmol L^{-1}) with the potential varied from -0.2 to 2.0 V was used to prepare a poly-L-cysteine film electrode. The assembling procedure was carried out by incubating the poly-L-cysteine film electrode in a gold nanorods solution over one night. After being washed carefully, a GNRs/poly-L-cysteine/GCE was fabricated for further studies.

2.4 Electrochemical measurements

Electrochemical determination of butyl hydroxy anisd was performed in a 0.1 mol L^{-1} phosphate buffer. Cyclic voltammetry was used to investigate the electrochemical behaviors of butyl

hydroxy anisd at the GNRs/poly-L-cysteine/GCE. After being accumulated under 0.1 V for 120 s, square wave voltammograms of butyl hydroxy anisd at the GNRs/poly-L-cysteine/GCE were recorded. The oxidation peak current was measured for the determination of butyl hydroxy anisd. The potential increment, amplitude, and frequency of square wave voltammetry are 4 mV, 25 mV, and 25 Hz, respectively.

2.5 Sample preparation

Oil samples were brought from local market. BHA was extracted by ethanol using ultrasonication. The typical procedure for the extraction of BHA was detailed as following: 5.633 g oil sample was dissolved into 30 mL ethanol, and was treated using ultrasonication. After two hours, the ethanol layer was detached, and was evaporated under vacuum. The residual was quantitatively transferred into a volumetric flask, and diluted to 10.00 mL with ethanol. The obtained sample solution was stored at ~ 4 ^{o}C, and diluted with phosphate buffer as measured by the GNRs/poly-L-cysteine/GCE.

3. RESULTS AND DISCUSSION

3.1 Morphological characterizations

Transmission electron microscopy was employed to characterize the morphology of the gold nanorods. As shown in Fig. 1 (a), nanorods with homogeneous length and diameter, and high aspect ratio were presented.

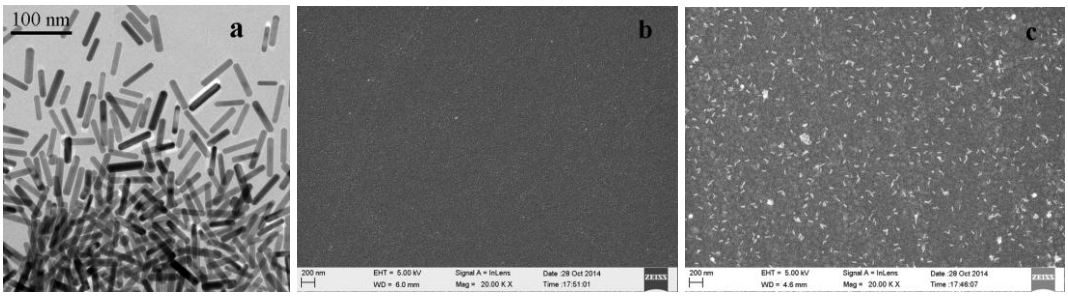

Figure 1. Characterizations of gold nanorods with transmission electron microscope (a), the poly-L-cysteine film electrode (a) and the GNRs/poly-L-cysteine*/GCE* (c) with scanning electron microscope.

The result demonstrates the successful preparation of gold nanorods with the seed mediating method. Cetyltrimethylammonium bromide has been used as a modifier to synthesize gold nanorods, thus existing on the surface of gold nanorods to provide a positively charged interface. The electrostatic repulsion produced by cetyltrimethylammonium bromide makes it possible to get

monodispersed gold nanorods in the aqueous solution. The scanning electron microscopic images of the poly-L-cysteine film electrode and the GNDs/poly-L-cysteine/GCE were shown in Fig. 1 b and Fig. 1 c, respectively. It was found that voltammetric scanning could promote the electrochemical polymerization of L-cysteine to form a smooth film on the glassy carbon electrode. Apparently we can see, based on an assembling procedure, that gold nanorods have also been modified onto the poly-L-cysteine film surface due to the covalent interaction between the thiol group and gold. Furthermore, the successful assembling of gold nanorods on the poly-L-cysteine film electrode surface can also be clarified by the color change from bright blue to gold yellow.

3.2 Electrochemical impedance spectroscopy

Electrochemical impedance spectroscopy was employed to study the interfacial properties of the GNRs/poly-L-cysteine/GCE.

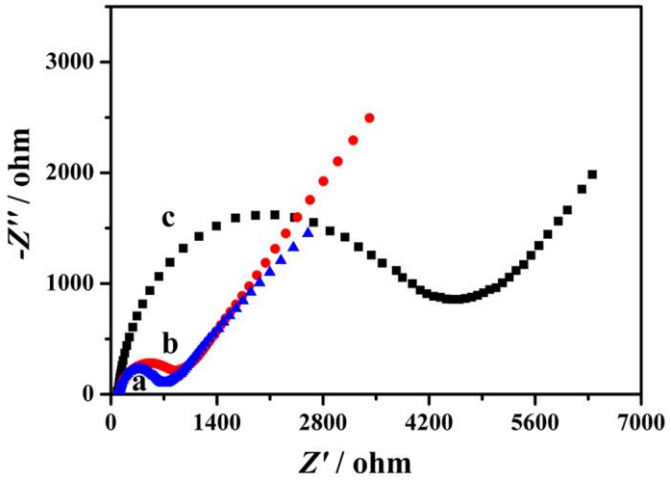

Figure 2. Nyquist plots of 5 mmol L^{-1} $K_3Fe(CN)_6/K_4Fe(CN)_6$ at the bare glassy carbon electrode (a), the GNRs/poly-L-cysteine/GCE (b) and the Poly-L-cysteine/GCE (c).

Fig. 2 shows the Nyquist plots of $K_3Fe(CN)_6/K_4Fe(CN)_6$ at the bare GCE (a), the GNRs/poly-L-cysteine/GCE (b) and the Poly-L-cysteine/GCE (c). The diameter of the semicircle obtained at high frequencies is corresponding to the charge transfer resistance (R_{ct}) of the electrode surface towards the electroactive probes. When L-cysteine was electrochemically deposited onto the glassy carbon electrode surface, the charge transfer resistance is obviously increased, meaning a retarded effect towards the redox reaction of $K_3Fe(CN)_6/K_4Fe(CN)_6$. Fortunately, after gold nanorods were successfully assembled on the poly-L-cysteine film surface, it is particularly significant that the charge transfer resistance decreased greatly. This decline is undoubtedly contributed to the superior properties of gold nanorods, such as good conductivity, high specific surface area, and the positively charged surface.

3.3 Cyclic voltammetric behavior of butyl hydroxy anisd

Voltammetric behaviors of 2.0×10^{-6} mol L^{-1} butyl hydroxy anisd at the GNRs/poly-L-cysteine/GCE (a), the poly-L-cysteine/GCE (c) and the bare GCE (d) were investigated with cyclic voltammetry.

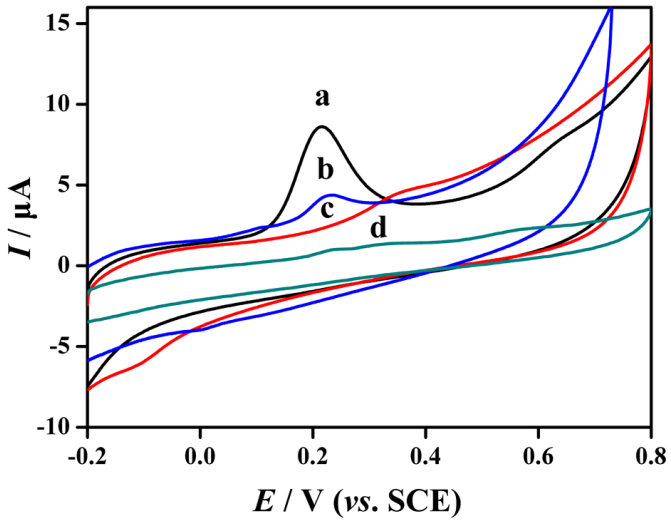

Figure 3. Cyclic voltammograms of 2.0×10^{-6} mol L^{-1} butyl hydroxy anisd at the GNRs/poly-L-cysteine/GCE (a, self-assembling), the GNRs/poly-L-cysteine/GCE (b, direct coating), the poly-L-cysteine/GCE (c) and the bare GCE (d).

As shown in Fig. 3, the voltammetric responses of butyl hydroxy anisd at the bare GCE and the poly-L-cysteine film electrode were indistinct. Obviously, at the GNRs/poly-L-cysteine/GCE, butyl hydroxy anisd presents a well-defined oxidation peak at 0.22 V. The oxidation peak current of butyl hydroxy ansid at 3the GNRs/poly-L-cysteine/GCE has been significantly enhanced with respect to those obtained from other electrodes. Although gold nanorods can be directly coated onto the poly-L-cysteine film surface to fabricate an electrode, the current response of butyl hydroxy ansid increased slightly (Fig. 3 b). In addition, in the reverse potential scanning, no reduction peak can be observed, meaning a totally irreversible oxidation process for butyl hydroxy ansid at the GNRs/poly-L-cysteine/GCE.

3.4 Optimization of experimental conditions

The dependence of the current response of 5.0×10^{-7} mol L^{-1} butyl hydroxy anisd on the pH value was investigated in the pH range from 7.0 to 11.0. The relationship between the peak currents and the pH values was shown in Fig. 4 (a).

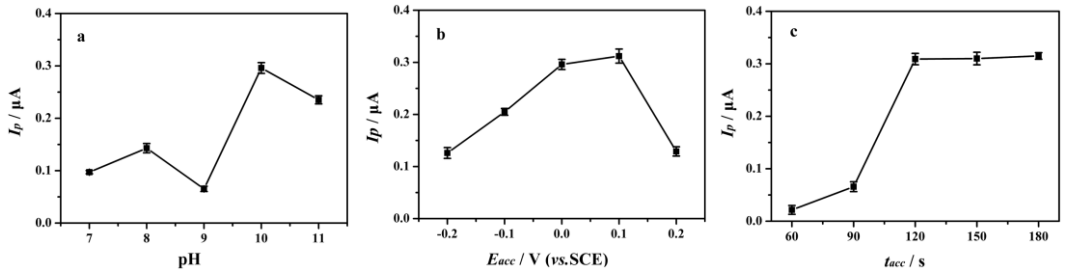

Figure 4. Influences of pH values (a), accumulation potential (b) and accumulation time on the current response of 5.0×10^{-7} mol L^{-1} butyl hydroxy anisd at the GNRs/poly-L-cysteine/GCE.

Although a sudden drop appeared at pH 9.0, an increasing trend in current response can also be seen from 7.0 to 10.0, and the maximum value was obtained at pH 10.0. Further increasing pH value from 10.0 to 11.0, the current response decreased inversely. At the pH value 10.0, butyl hydroxy anisd has been almost completely deprotonated to be an anion. As a result, there be an electrostatic attraction between butyl hydroxy anisd and the positively charged CTAB, resulting in an enhanced effect on the peak current response. Therefore, a phosphate buffer at pH 10.0 was selected for butyl hydroxy anisd determination.

In order to improve the sensitivity of the GNRs/poly-L-cysteine/GCE, the effects of the accumulation potential as well as the accumulation time on the oxidation peak current of butyl hydroxy anisd were examined. It can be seen from Fig. 4 (b), as the accumulation potential varied from -0.2 to 0.1 V, the oxidation peak current increased gradually, and the maximum value was achieved at 0.1 V. Then, a significant decrease was observed with further increasing the accumulation potential from 0.1 V to 0.2 V. The electrochemical oxidation of butyl hydroxy anisd in the accumulation process might be the reason for the current declining. The oxidation peak current of butyl hydroxy anisd is also positively related to the accumulation time. As presented in Fig. 4 (c), the oxidation peak current dramatically increased with the accumulation time increasing from 60 s to 120 s. When the accumulation time was controlled in the range from 120 s to 180 s, the peak current changed slightly, suggesting that the accumulation of butyl hydroxy anisd to the GNRs/poly-L-cysteine/GCE surface has reached a saturation state. Thus, the accumulation process for butyl hydroxy anisd was performed under an accumulation potential of 0.1 V for 120 s.

3.5 Reproducibility, selectivity and stability

To investigate the fabrication reproducibility, five GNRs/poly-L-cysteine/GCEs, which were prepared independently, were used to determine 5.0×10^{-7} mol L^{-1} butyl hydroxy anisd respectively. The average relative standard deviation for the five separated determinations is 4.46%, meaning a satisfied reproducibility for the fabrication of GNRs/poly-L-cysteine/GCEs. Unfortunately, using an identical GNRs/poly-L-cysteine/GCE for the butyl hydroxy anisd determination, the oxidation peak current decreased evidently, indicating that it is suitable to be employed as a disposable sensor. The selectivity of the GNRs/poly-L-cysteine/GCE was evaluated by the addition of potential interfering substances

(ascorbic acid, phenol, metal cations and inorganic acid anions) in a standard solution containing 2.0×10^{-7} mol L^{-1} butyl hydroxy anisd. When the concentration of interferents was 2.0×10^{-6} mol L^{-1}, the obtained current signals were compared with those in the absence of each possible interferent (SD < 5.0%), meaning these compounds do not significantly interfere with the determination of butyl hydroxy anisd using the developed method. The stability was studied by storing the GNRs/poly-L-cysteine/GCE at room temperature for three weeks. Subsequently, the electrode was used for the determination of 5.0×10^{-7} mol L^{-1} butyl hydroxy anisd. It was found that the current response can retain 93.5% of its original response, shows good stability.

3.6 Analytical characteristics

Square wave voltammetry was used to evaluate the analytical features of the developed method. Fig. 5 (A) shows the typical square wave voltammograms of butyl hydroxy anisd at the GNRs/poly-L-cysteine/GCE.

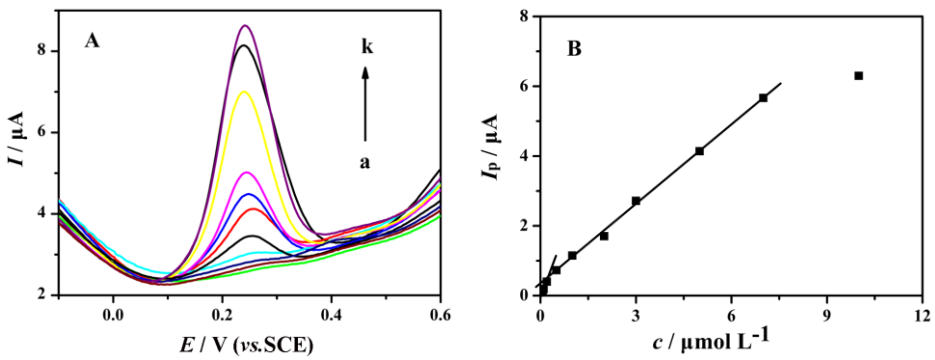

Figure 5. Square wave voltammograms of butyl hydroxy anisd at the GNRs/poly-L-cycteine/GCE with different concentrations (A) and the calibration curve for butyl hydroxy anisd determination (B). (From curve a to k, butyl hydroxy anisd concentration varied from 0.05 to 10.0 μmol L^{-1}).

It can be seen from Fig. 5 (B) that the oxidation peak current (*I*p) was proportional to butyl hydroxy anisd concentration (*c*) in the range from 0.05 to 0.2 and 0.2 to 7.0 μmol L^{-1}. The linear equations can be expressed as *I*p (μA) = 2.29 *c* (μmol L^{-1}) + 0.0126 (R=0.994) and *I*p (μA) = 0.760 *c* (μmol L^{-1})+ 0.345 (R=0.998), respectively. The detection limit is calculated to be 8.5×10^{-9} mol L^{-1}. There are two slopes for the calibration curves, meaning the GNDs/poly-L-cysteine/GCE presents different sensitivity towards butyl hydroxy anisd at different concentration. At low concentration, the active sites provided for the accumulation of butyl hydroxy anisd were sufficient, thus exhibiting high sensitivity. When the butyl hydroxy anisd concentration increasing, the amount of active sites is relatively small and shows some restricted effects on the accumulation of butyl hydroxy anisd to the electrode surface. As a result, a low sensitivity appeared at high concentrations.

3.7 Practical application

To verify the validity of the developed method, the GNRs/poly-L-cysteine/GCE was applied for the determination of butyl hydroxy anisd in oil samples. No oxidation peaks were observed when these oil samples were analyzed, meaning no butyl hydroxy anisd is in these samples or the concentration of butyl hydroxy anisd is lower than the detection limit. Thus, a standard addition method was used to determine butyl hydroxy anisd. As can be seen from Table 1, the results obtained with the developed method is accurate, due the good recoveries ranged from 94.5% to 102.5%. Therefore, GNRs/poly-L-cysteine/GCE is suitable to assay butyl hydroxy anisd in real matrix samples.

Table 1. Results for the determination of BHA in oil samples using the GNRs/poly-L-cysteine/GCE electrode.

Sample	Added (μmol L^{-1})	Found (μmol L^{-1})	Recovery (%)	RSD (%)
		0.485	97.0	
1	0.5	0.512	102.4	3.04
		0.487	97.4	
		1.98	99.0	
2	2	2.05	102.5	4.06
		1.89	94.5	

4. CONCLUSIONS

We have successfully synthesized a nanointerface based on the assembling of gold nanorods onto a poly-L-cysteine film electrode surface. The prepared nanointerface exploits the synergistic effects of the gold nanorods and poly-L-cysteine film, and exhibits enhanced effects on the electrochemical sensing performances towards butyl hydroxy anisd. Voltammetric behaviors of butyl hydroxy anisd on the GNRs/poly-L-cysteine/GCE were investigated. A voltammetric method was developed for the butyl hydroxy anisd determination, and practically used in oil samples. It seems that the method developed can be recommended for practical analysis.

ACKNOWLEDGEMENTS
The authors gratefully acknowledge the financial supports from National Natural Science Foundation of China (No.21275166), Natural Science Foundation of Hubei Province (No.2015CFA092), Science and Technology Innovation Foundation for Student in South-Central University for Nationalities (No. GXX14201), Research foundation of General Administration of Quality Supervision, Inspection, and Quarantine of the People's Republic of China (No. 2013Qk286), and Open Foundation of Hubei key laboratory of purification and application of plant anti-cancer active ingredients, Hubei University of Education (No. HLPAI2014007).

References

1. R. Guerra, *Chemosphere*, 44 (2001) 1737–1747.
2. B. Poljsak, R. Dahmane and A. Godic, *J. Cosmet. Laser Ther*., 15 (2013) 107–113.

3. I. Gulcin and S. Beydemir, *Mini-Rev. Med. Chem.*, 13 (2013) 408–430.
4. M. Carocho and I.C.F.R. Ferreira, *Food Chem. Toxicol*., 51 (2013) 15–25.
5. D.B. Clayson, F. Iverson, E. Lok and C. Rodrigues, *Food Chem. Toxicol*., 24 (1986) 1171–1182.
6. G.J. van Esch, *Food Chem. Toxicol*., 24 (1986) 1063–1065.
7. S.J. Xu, F.N. Chen, M. Deng and Y.Y. Sui, *Luminescence*, 29 (2014) 1027–1032.
8. J.Y. Wang, H.L. Wu, Y. Chen, M. Zhai, X.D. Qing and R.Q. Yu, *Talanta*, 116 (2013) 347–353.
9. C. Liu, J. Wang and Y.L. Yang, *Anal. Meth*., 6 (2014) 6038–6043.
10. P. Biparva, M. Ehsani and M. R. Hadjmohammadi, *J. Food Compos Anal*., 27 (2012) 87–94.
11. J.I. Cacho, N. Campillo, P. Vinas and M. Hernandez-Cordoba, *Food Addit. Contam*. A, 32 (2015) 665–673.
12. R.A. Medeiros, B.C. Lourenção, R.C. Rocha-Filho and O. Fatibello-Filho, *Anal. Chem*., 82 (2010) 8658–8663.
13. K.H.G. Freitas and O. Fatibello-Filho, *Talanta*, 81 (2010) 1102–1108.
14. M.D. Raymundo, M.M.D. Paula, C. Franco and Fett R, *LWT-Food Sci. Techol*., 40 (2007) 1133–1139.
15. S. Michalkiewicz, M. Mechanik and J. Malyszko, *Electroanal*., 16 (2004) 588–595.
16. Y.N. Wang, W.T. Wei, C.W. Yang and M.H. Huang, *Langmuir* 29 (2013) 10491–10497.
17. A. Thete, O. Rojas, D. Neumeyer, J. Koetzb and E. Dujardin, *RSC Adv*., 3 (2013) 14294–14298.
18. D.A. Giljohann, D.S. Seferos, W.L. Daniel, M.D. Massich, P.C. Patel and C.A. Mirkin, *Angew. Chem. Int. Ed*., 49 (2010) 3280–3294.
19. W.Q. Bai, H.Y. Huang, Y. Li, H.Y. Zhang, B. Liang, R. Guo, L.L. Du and Z.W. Zhang, *Electrochim. Acta*, 117 (2014) 322–328.
20. D.J. Lin, J. Wu, H.X. Ju and F. Yan, *Biosens. Bioelectron*., 45 (2013) 195–200.
21. C.G. Wang, J.J. Chen, T. Talavage and J. Irudayaraj, *Angew. Chem. Int. Ed*., 48 (2009) 2759–2763.